International Journal of Hydrogen Energy 250 (2026) 156052

Contents lists available at ScienceDirect

International Journal of Hydrogen Energy

journal homepage: www.elsevier.com/locate/he

Autoignition of ammonia-hydrogen mixtures under engine relevant conditions - second law analysis

D.N. Rrustemi [a,*], T. Megaritis [a], L.C. Ganippa [b]

[a] Department of Mechanical and Aerospace Engineering, Brunel University of London, Uxbridge, London, UB8 3PH, United Kingdom
[b] Department of Aerospace and Aircraft Engineering, School of Engineering, Kingston University, London, SW15 3DW, United Kingdom

ARTICLE INFO

Keywords:
Ammonia ignition
Autoignition delay time
Exergy destruction
Hydrogen

ABSTRACT

Hydrogen addition can enhance ammonia reactivity and improve its ignition characteristics. This study investigates the fundamental mechanisms governing ignition improvement in ammonia and hydrogen mixtures by quantifying exergy destruction during autoignition at a pressure of 5 MPa, temperature of 900 K, and equivalence ratios of 0.5 to 1. Exergy destruction of each elementary reaction is quantified using species production rates and Gibbs free energy changes. Results show that hydrogen addition significantly increases instantaneous exergy destruction due to enhanced radical generation and chain-branching reactions. However, the total exergy destruction decreases by 19% and 30% for hydrogen addition levels of 40% and 60%, respectively, primarily due to the shorter ignition delay time, which reduces the duration available for irreversible processes. This is further reflected in decreased exergy destruction from NH_X oxidation and NO_X chemistry, while exergy destruction from radical growth reactions increases due to enhanced H and OH production.

1. Introduction

Recently, ammonia has been recognized as a potential hydrogen carrier due to its ease of storage and transportation [1]. It can also be used directly as a fuel in combustion systems [2]. However, engines operating on neat ammonia may suffer from lower thermal efficiency and narrower operating ranges compared to conventional hydrocarbon fuels, mainly due to ammonia's lower flame speed and combustion temperature [3]. The addition of hydrogen has been shown to increase the flame speed, thereby improving the combustion stability of ammonia mixtures [4]. This effect becomes more pronounced when the hydrogen fraction in ammonia mixtures exceeds 30% by volume [5]. The addition of hydrogen has been shown to promote ammonia decomposition and increase in the pool of reactive radicals such as H and OH species [6]. Significant amount of research has been devoted to developing detailed kinetics to understand the influence of hydrogen-enriched ammonia mixtures [7]. Hydrogen enrichment accelerates the overall ammonia reaction rates; however, the coupling between hydrogen and ammonia oxidation pathways becomes increasingly complex under fuel-rich and high-pressure conditions, where hydrogen regeneration and unimolecular decomposition of N_2H_2 play significant roles [8]. A comprehensive chemical kinetic mechanism was developed in Ref. [9] for hydrogen with ammonia mixtures to predict ignition delay times at high temperatures, based on shock tube experimental data given in Refs. [10,11,12]. Since it is evident that hydrogen addition improves significantly the reactivity of ammonia mixtures, it is important to investigate the underlying fundamental thermo-chemical mechanisms that promotes its effects and its maximum potential. The second law of thermodynamics provides insights to destruction mechanisms through the concept of exergy, which is defined as the maximum theoretical useful work that can be extracted from a system [13,14]. Exergy analysis allows the evaluation of the performance of internal combustion engines by identifying and quantifying the thermodynamic destruction due to the irreversiblities [15,16]. In flames, exergy destruction can occur through thermal conduction, viscous dissipation, and mass diffusion [17]. During the burning of the reactive mixture within the combustion chamber, exergy destruction mainly arises from the chemical reactions initiating combustion and subsequent flame propagation [18]. Hydrogen addition to ammonia mixtures has been found to reduce exergy destruction, mainly by decreasing exergy destruction associated with reduction of heat conduction and increase of mass diffusion. The chemical kinetic mechanisms contributing to exergy destruction in ammonia fuelled internal combustion engine could be classified into three groups: ammonia pyrolysis, ammonia oxidation,

* Corresponding author. Department of Mechanical and Aerospace Engineering, Brunel University of London, Uxbridge, London, UB8 3PH, United Kingdom.
E-mail addresses: Dardan.Rrustemi@brunel.ac.uk (D.N. Rrustemi), Thanos.Megaritis@brunel.ac.uk (T. Megaritis), Lionel.Ganippa@brunel.ac.uk (L.C. Ganippa).

https://doi.org/10.1016/j.ijhydene.2026.156052
Received 24 February 2026; Received in revised form 3 June 2026; Accepted 11 June 2026
Available online 19 June 2026
0360-3199/© 2026 The Author(s). Published by Elsevier Ltd on behalf of Hydrogen Energy Publications LLC. This is an open access article under the CC BY license (http://creativecommons.org/licenses/by/4.0/).

and hydrogen oxidation. The irreversibility in chemical reactions are accounted for up to three-quarters of the total entropy generation in lean ammonia with hydrogen mixtures, and the reactions with the highest contributions to exergy destruction were identified in Ref. [19] as $NH_3+OH=NH_2+H_2O$, $H+O_2=HO_2$, $H_2+OH=H+H_2O$, and $NH_2+NO=H_2O+N_2$. Exergy destruction occurs primarily during the low- and high-temperature reaction stages, where chemical reactions lead to significant irreversibility, resulting in a reduction in the system's available free energy [20]. Therefore, it is crucial to investigate the reactions responsible for exergy destruction in ammonia with hydrogen mixtures under elevated engine relevant pressures to better understand the fundamental mechanisms of exergy destruction during ignition. For example, the second law of thermodynamics has previously been applied to natural gas–air mixtures to investigate the effects of various constant-volume boundary conditions, such as equivalence ratio, temperature, and pressure, under different levels of hydrogen addition [21]. The hydrogen addition reduces exergy destruction during the ignition of methane mixtures, primarily by increasing the concentrations of H atoms and OH radicals [22]. Zhang et al. [23] quantified the reaction-resolved exergy destruction during the autoignition of dimethyl ether blended with methanol and ethanol in an adiabatic constant-volume system. The elementary reactions were classified into four groups as fuel-series, fuel-fragmentation, H_2O_2 loop, and H_2–O_2 reaction stages, and the trade-off in exergy destruction between these groups was analysed across varying fuel composition, equivalence ratio, pressure and temperature. A similar reaction-resolved exergy approach was adopted in Ref. [24] to isolate the dilution, thermal, and chemical effects of CO_2 addition on the autoignition of n-heptane and iso-octane, revealing that the dilution effect reduced exergy destruction in the H_2O_2 reaction group, the thermal effect increased exergy destruction, and the chemical effect reduced exergy destruction in the H_2–O_2 reaction group for both fuels. These studies demonstrated that classifying elementary reactions into distinct groups reveals which chemical pathways are responsible for the majority of exergy destruction. While reaction-resolved exergy destruction analysis has been applied to various hydrocarbons [23,24] and hydrogen-enriched methane autoignition processes [21], the elementary reaction exergy contribution of ammonia-hydrogen mixtures under high-pressure engine-relevant conditions remains not available in the literature. This study quantifies the exergy destruction during the autoignition of ammonia-hydrogen mixtures by evaluating the exergy destruction associated with each elementary reaction, based on species production rates and the corresponding Gibbs free energy changes, thereby providing reaction-resolved insight into the thermodynamic irreversibility of ammonia-hydrogen autoignition under high-pressure engine-relevant conditions.

2. Methodology

2.1. Autoignition delay time

The autoignition delay time of ammonia with different hydrogen addition levels and equivalence ratios was investigated using zero-dimensional constant-volume reactor simulations in Chemkin-Pro. The model assumes an isolated system with no heat and work interactions, and is represented as an adiabatic, closed, constant-volume reactor. The simulations were performed at elevated pressures and temperatures representative of engine-relevant conditions using the detailed chemical kinetic mechanism of [9]. The homogeneous reactor model solves the coupled species conservation and energy equations to predict the temporal evolution of temperature, pressure, and species concentrations during autoignition, based on the net contribution of all forward and reverse elementary reactions. The employed mechanism consists of 312 elementary reactions and accurately captures the chemical pathways governing ammonia and hydrogen autoignition under the conditions presented in Table 1.

Table 1
Initial conditions.

Parameter	Value
Hydrogen addition (% by volume)	0 to 60
Equivalence ratio (−)	0.5 to 1
Pressure (MPa)	5
Temperature (K)	900

2.2. Exergy destruction due to autoignition

Entropy is a thermodynamic property that quantifies the degree of disorder or irreversibility within a system. Entropy could be generated by irreversible processes such as unrestrained chemical reactions, friction, heat transfer across different temperature zones, and mixing of different gases [25]. In combustion systems, chemical reactions represent the dominant source of entropy generation. Based on the Gouy-Stodola theorem, entropy generation is directly proportional to exergy destruction, which is defined as the thermodynamic work potential permanently lost due to irreversible processes [26]. For an adiabatic, closed, constant-volume system with no heat or work transfer within the system boundary, the entropy generation S_{gen} could be formulated as:

$$S_{gen} = -\sum_k \frac{\mu_k \omega_k}{T} \tag{1}$$

where μ is the chemical potential per mole, ω is the moles production rate and the subscript k refers to corresponding specie of interest. The chemical potential of each species was calculated as the difference between the species-specific enthalpy h_k and the temperature T multiplied by the species entropy s_k:

$$\mu_k = h_k^0 - Ts_k \tag{2}$$

The entropy of each specie k was calculated as:

$$s_k = s_k^0 - Rln\left(\frac{x_k P}{P_0}\right) \tag{3}$$

The term s_k^0 is the entropy species at the reference state which corresponds to pressure and temperature of 0.1 MPa and 298.15 K, respectively. The superscript *0* is used to denote the standard state. The specific heat capacity at constant pressure c_p^0, specific enthalpy h^0, and specific entropy s^0 are calculated using Eqs. (4)–(6) to determine unburned and burned mixture properties.

$$\frac{c_p^0(T)}{R} = a_1 + a_2T + a_3T^2 + a_4T^3 + a_5T^4 \tag{4}$$

$$\frac{h^0(T)}{RT} = a_1 + \frac{a_2T}{2} + \frac{a_3T^2}{3} + \frac{a_4T^3}{4} + \frac{a_5T^4}{5} + \frac{a_6}{T} \tag{5}$$

$$\frac{s^0(T)}{R} = a_1lnT + a_2T + \frac{a_3T^2}{2} + \frac{a_4T^3}{3} + \frac{a_5T^4}{4} + a_7 \tag{6}$$

The internal energy is given by:

$$u^0 = h^0 - RT \tag{7}$$

Two ranges of temperature are considered for the values of the coefficients a for NH_3, H_2, O_2, N_2 and H_2O, the lower range (300-1000 K) is used for the unburned mixture properties, while the higher range (1000-5000 K) is used for the burned mixture properties. The coefficients used to calculate the parameters of Eqs. (4)–(6) are taken from Ref. [9]. The molar production rate ω_k for each species was obtained for the 312 reaction kinetic mechanisms accounting for both the forward and reverse reaction rates under instantaneous thermodynamic conditions as discussed in Ref. [9]. The ignition delay time sensitivity coefficient was calculated using:

$$S_{\tau_i} = \frac{k_i}{\tau}\frac{\partial \tau}{\partial k_i} \quad (8)$$

where τ is the ignition delay time and k_i is the pre-exponential factor of reaction i. A positive sensitivity coefficient indicates that the reaction promotes autoignition by decreasing the ignition delay time, while a negative coefficient indicates an inhibiting effect.

3. Results and discussion

3.1. Chemical kinetic mechanism validation and sensitivity analysis

The autoignition delay time, IDT, for the mixture compositions of ammonia with hydrogen was in an adiabatic, constant-volume chamber was calculated using Chemkin-Pro based on the chemical reaction kinetic mechanism of [9]. The autoignition delay time is defined as the time interval corresponding to attain the peak rate of change of pressure due to autoignition at a defined ambient condition. The mixture composition details are presented in Table 1. Fig. 1 shows a comparison between the simulated and experimental IDT values from the shock tube data of [27]. It can be seen that the chemical kinetic mechanism accurately predicts the decrease in IDT with increasing temperature, which is consistent with the Arrhenius dependence of reaction rates [28]. The chemical kinetic mechanism of [9] was reported to provide the best agreement with experimental autoignition delay times of ammonia-hydrogen mixtures at high-pressure and intermediate-temperature conditions relevant to this study, when compared with various available mechanisms [29]. Additionally, the simulated IDT values show that increasing the hydrogen addition percentage leads to a significant decrease in the IDT of the ammonia mixture. At a temperature of 1100 K, the IDT was reduced by nearly fivefold for the ammonia mixture with 50% hydrogen addition compared to that with 20% hydrogen addition. This reduction of IDT is attributed to hydrogen's higher diffusivity, and greater radical-generation capability compared to ammonia [30]. This trend of decrease in IDT due to hydrogen addition was accurately captured by the chemical kinetic reaction mechanism for ammonia mixtures presented in Ref. [9]. Overall, the simulated IDT values showed good agreement with the experimental but slight deviations were observed for the ammonia mixture containing 50% hydrogen addition. The deviation between the simulated and experimental ignition delay times in the temperature range of 1100–1300 K for ammonia with 50% hydrogen addition observed in Fig. 1 is consistent with the limitations discussed in Ref. [31] and is attributed to uncertainties in the HO_2 reaction chemistry at intermediate temperatures. However, the predictions under these conditions could be improved by updating rate coefficients for HO_2 reactions chemistry [27]. In this case, the kinetic reaction mechanism underpredicts the experimental IDT values in the temperature range of 1100 to 1300 K. Fig. 2 shows the IDT sensitivity analyses of neat ammonia at different hydrogen addition percentages at a temperature and pressure of 1000 K and 5 MPa. The positive sensitivity coefficients indicate the reactions that increase the mixture reactivity, whereas the negative sensitivity coefficients indicate the reaction that decrease the mixture reactivity. It can be seen that for the neat ammonia mixture at elevated pressure and temperature, the reactivity of the mixture increases due to hydrogen abstraction and ammonia decomposition through the formation of the H_2NO radical produced from the reactions $NH_2+NO_2=H_2NO+NO$ and $HO_2+NH_2=H_2NO+OH$. The H_2NO then reacts with O_2 to produce the HNO molecule, which is significant in increasing the mixture reactivity. With the addition of 20% hydrogen, the reactions that increase mixture reactivity shift from $NH_2+NO_2=H_2NO+NO$ and $HO_2+NH_2=H_2NO+OH$ to $H_2O_2(+M)=2OH(+M)$. The reaction $H_2O_2(+M)=2OH(+M)$ significantly increases the radical pool with OH radicals, with H_2O_2 being produced from ammonia decomposition via $HO_2+NH_3=H_2O_2+NH_2$. Additionally, the NH_2 radicals produced from ammonia decomposition through $H+NH_3=H_2+NH_2$ further increases the mixture reactivity via $NH_2+NO_2=H_2NO+NO$ and $HO_2+NH_2=H_2NO+OH$. It can be seen that for neat ammonia, the major consumption pathway of NO was through the reaction $NH_2+NO=H_2O+N_2$, which led to the formation of end-of-combustion products such as H_2O and N_2, thus acting as a chain-termination reaction that decreases the reactivity of the mixture [32]. Similarly, the reactions $NH_3+OH=H_2O+NH_2$ and $NH_2+NO_2=H_2O+N_2O$ contributed to lower mixture reactivity for both neat ammonia and ammonia with 20% hydrogen addition. The formation of H_2O reduces reactivity by increasing the heat capacity of the mixture and enhancing third-body collision effects, thereby suppressing the temperature rise and inhibiting chain-branching reactions. It can be seen from Fig. 2 that for ammonia with 20% hydrogen addition, the reactions $H+O_2(+M)=HO_2(+M)$ and $H+O_2(+N_2)=HO_2(+N_2)$ decrease the reactivity significantly compared to neat ammonia. This occurs due to the presence of a larger pool of H radicals, which enhances the formation of HO_2 through three-body recombination reactions. HO_2 can react with NH_2 to regenerate NH_3, thereby suppressing ammonia oxidation and contributing to increased ammonia slip under intermediate-temperature combustion conditions.

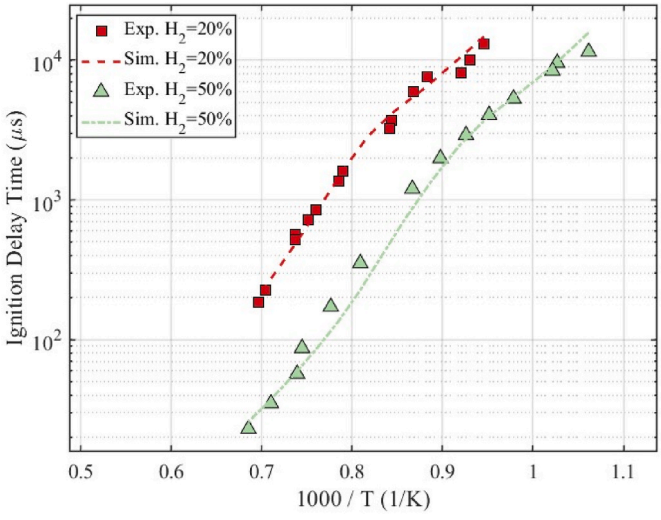

Fig. 1. Simulated ammonia IDT compared to experimental values of [27] at various hydrogen addition percentages at different temperatures (P = 1.6 MPa, ∅ = 1).

3.2. Exergy destruction due to autoignition

Based on the methodology described in Section 2.2, the exergy destruction during the autoignition of ammonia with hydrogen mixtures was quantified by calculating the exergy destruction associated with each elementary reaction using the species production rates and corresponding Gibbs free energy changes. The analysis was applied to 312 reactions of the ammonia with hydrogen addition based on the chemical reaction mechanisms of [9], that provides the contribution of each individual reaction to the overall exergy destruction caused by the autoignition of the mixture. Fig. 3 show the temperature and the total exergy destruction rate for stoichiometric mixture of ammonia with different hydrogen addition percentages maintained at an initial pressure of 5 MPa and temperature of 900 K. The pressure of 5 MPa and temperature of 900 K were selected to represent the in-cylinder conditions at the onset of autoignition in a homogeneous charge compression ignition (HCCI) engine [33]. As it can be seen from Fig. 3a–c the addition of hydrogen to the ammonia mixture increased the reactor temperature, due to hydrogen's higher diffusivity, and higher chemical reactivity compared to ammonia [34]. The instantaneous exergy destruction rate peak increased by 47% and 97% for 40% and 60% hydrogen addition to

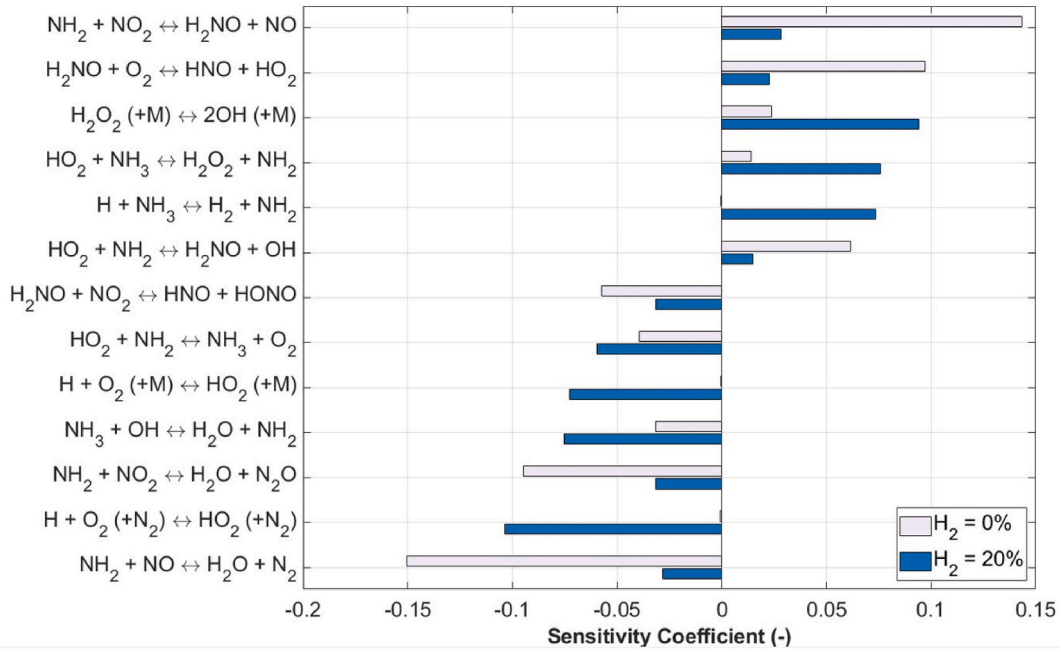

Fig. 2. Autoignition delay time sensitivity analyses for stoichiometric ammonia mixture with different hydrogen addition percentages ($T_{in} = 1000$ K, P = 5 MPa, ∅ = 1).

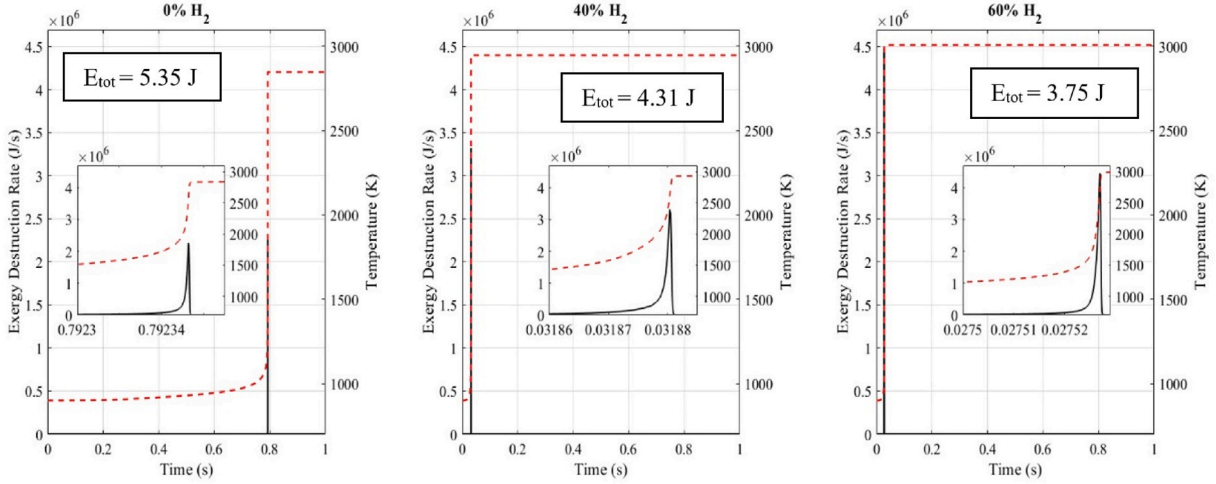

Fig. 3. Total destroyed exergy rate and temperature for a) neat ammonia, b) ammonia with 40% hydrogen addition percentage, and c) ammonia with 60% hydrogen addition percentage (P = 5 MPa, $T_{in} = 900$ K, ∅ = 1).

the ammonia mixtures, indicating a significant increase in the reaction rates. However, even though the ammonia ignition exergy destruction rate peak increased, the total cumulative exergy destruction decreased by 19% and 30% for 40% and 60% hydrogen addition, respectively. This was due to shorter ignition delay time caused by the higher reactivity of hydrogen and its faster chemical kinetics, which reduced the total time duration until ignition and the associated time available for irreversible processes and entropy generation. This was due to shorter ignition delay time caused by the higher reactivity of hydrogen and its faster chemical kinetics, which reduced the total time duration until ignition and the associated time available for irreversible processes and entropy generation. As seen from Fig. 4, for neat ammonia the dominant exergy destruction reactions are associated with NH_x-NO_x chemistry, where the oxidation proceeds via multiple intermediate steps with relatively slow radical generation pathways. With increasing hydrogen addition, the dominant exergy destruction shifts progressively toward hydrogen-related chain-branching reactions indicating the faster radical generation pathways that characterise hydrogen oxidation. To further investigate the exergy destruction due to the autoignition of ammonia mixtures with various hydrogen addition percentages, the five most influential reactions on the exergy destruction for various cases are shown in Fig. 4. It can be seen that for neat ammonia the main reactions contributing to exergy destruction are $NH_2+NO=H_2O+N_2$, $NH_3+OH=H_2O+NH_2$ and $NNH+O_2=HO_2+N_2$. These reactions are exothermic and form stable products such as H_2O and N_2, resulting in a large Gibbs free energy difference between reactants and products, and consequently higher entropy generation. The reactions $NH_2+NO=H_2O+N_2$ and $NNH+O_2=HO_2+N_2$ proceed mainly in the forward direction under combustion conditions, with minimal backward reactions, further increasing the entropy difference between products and reactants. These reactions destroy exergy primarily by producing thermodynamic irreversibility through the formation of stable

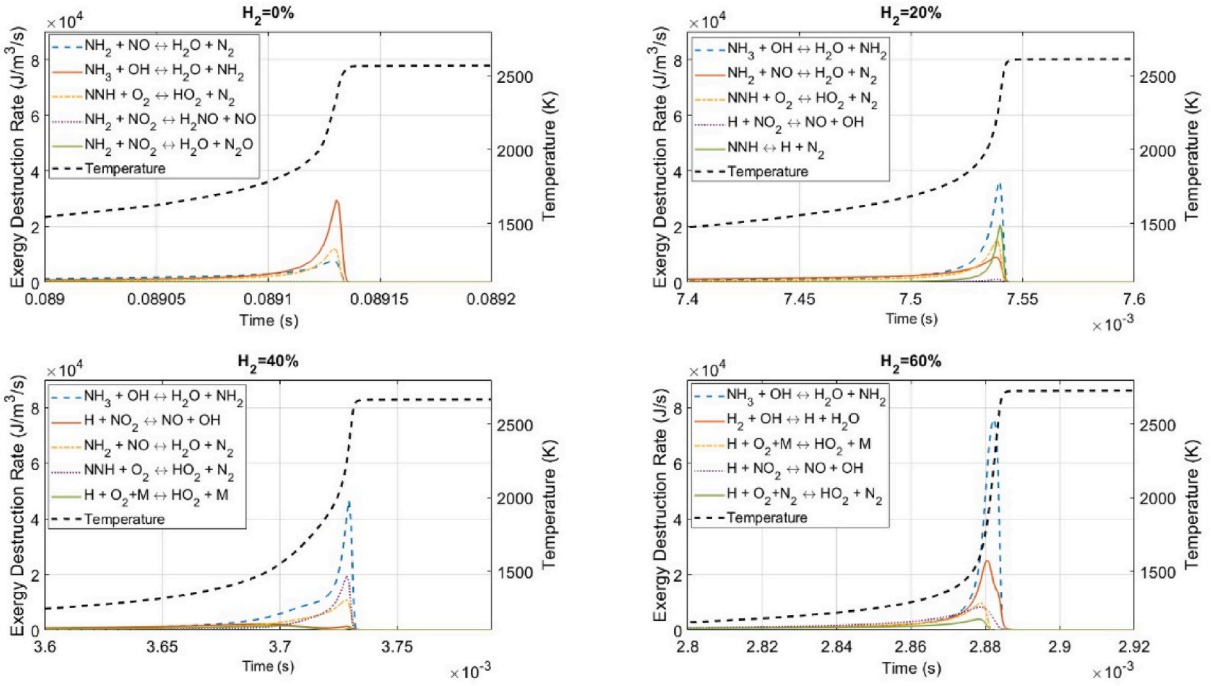

Fig. 4. Main five reactions on exergy destruction of the ignition of ammonia with various hydrogen addition percentages (P = 5 MPa, T_{in} = 900 K, ∅ = 1).

molecules such as N_2, N_2O, and NO. In addition, the formation of H_2O contributes to energy redistribution among third bodies, enhancing local irreversibility during these exothermic reactions. Moreover, since these reactions are closely linked to NO_x and OH formation chemistry, it increases thermodynamic irreversibility through chain-branching processes. Note that no boundary work was produced by the system, and no exergy was transferred through heat transfer. This allowed isolation of the effects of the chemical reactions on exergy destruction during the autoignition of ammonia with hydrogen mixtures. Even when more than 40% hydrogen was added to the ammonia combustible mixture, the reaction that contributed most to exergy destruction was still NH_3+OH=H+H_2O+NH_2. However, the radical-generating pathways became more dominant. The enhanced production of highly reactive H and OH radicals accelerated the oxidation kinetics, leading to greater chemical irreversibility and, consequently, a higher overall exergy destruction rate. This leads to a larger radical pool that increase the mixture reactivity. This larger pool of H and OH radicals shift the chemistry away from the slower NH_x and NO_x reaction routes, thereby reducing the amount of exergy destruction due to the autoignition. Although the instantaneous exergy destruction rate increases due to the faster reactions, the total cumulative exergy destruction decreases because the combustion occurs over a significant shorter time.

3.3. Ammonia reaction pathways and exergy destruction

To identify the most influential chemical reactions, the ammonia with hydrogen reactive mixture was divided into four main groups. These groups were determined as shown in Table 2 and the dominant reactions contributing to exergy destruction during the autoignition of ammonia mixtures with varying hydrogen addition percentages are shown in Fig. 5. The first group consists of the ammonia fuel initiation, decomposition and N–N intermediate reactions, including NH_3+OH=H_2O+NH_2, N_2H_2+NH_2=NH_3+NNH, NNH=H+N_2, and NNH+O_2=HO_2+N_2. The second group corresponds to NH_X oxidation and NO_X chemistry and includes reactions such as NH_2+NO=H_2O+N_2, NH_2+NO_2=H_2NO+NO, NH_2+NO_2=H_2O+N_2O, NH_3+NO=HNO+NH_2, and HNO+O_2=HO_2+NO. The third group comprises radical growth reactions, including propagation and branching processes, represented by H_2+OH=H+H_2O, H+HO_2=2OH, H+O_2(+M)=HO_2(+M), H+O_2(+N_2)=HO_2(+N_2), NH_2+OH=H+H_2NO, and H+NO_2=NO+OH. Finally, the fourth group represents radical termination reactions, consisting of HO_2+NH_2=NH_3+O_2. These classifications are used to discuss the parametric study of exergy destruction during the autoignition of ammonia with different hydrogen fractions under various constant volume initial conditions. Furthermore, Fig. 5 also shows exergy destruction during the autoignition of ammonia with different hydrogen addition percentages, effect discussed in Section 3.2.1.

Table 2
Classification of dominant reaction groups during ammonia and hydrogen autoignition.

Group	Category
1	Ammonia initiation, decomposition and N–N intermediate reactions
2	NH_X oxidation and NO_X chemistry
3	Radical growth (propagation and branching)
4	Radical termination

3.3.1. Effect of hydrogen addition

Fig. 6 shows the total exergy destroyed during ignition and its distribution among the four reaction groups defined in Section 3.2. The results indicate that increasing the hydrogen fraction in ammonia mixtures with various hydrogen addition percentages reduces the total exergy destruction associated with autoignition. The total cumulative exergy destruction decreased from 5.35 J for neat ammonia to 4.83 J, 4.31 J, and 3.75 J for 20%, 40% and 60% hydrogen addition, respectively. The reduction of exergy destruction of ammonia mixture ignition with hydrogen addition was mainly due to the reactions of NH_X oxidation and NO_X chemistry (group 2). The reduction in NH_X–NO_X exergy destruction with hydrogen addition results from two coupled effects: a dilution effect, whereby higher hydrogen addition reduces the ammonia concentration and hence the availability of NH_X species, and a chemical effect, whereby the expanded H/OH radical pool shifts. The oxidation pathways due to dilution effect associated with NH_X–NO_X shifts toward chemical effect for faster chain-branching reactions. The exergy destruction due to reactions of group 2 decreased by 42%, 73%, and

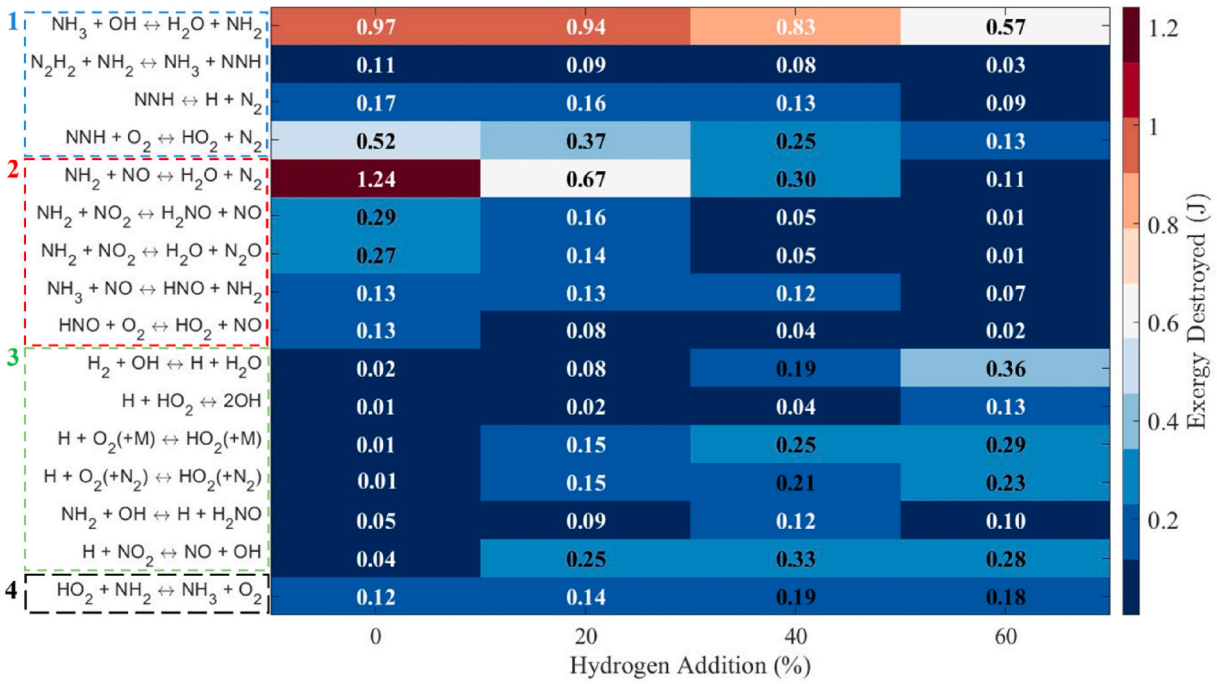

Fig. 5. Exergy destroyed by various reactions during the autoignition of ammonia-hydrogen mixtures with various hydrogen addition percentages (P = 5 MPa, T = 900 K, ∅ = 1).

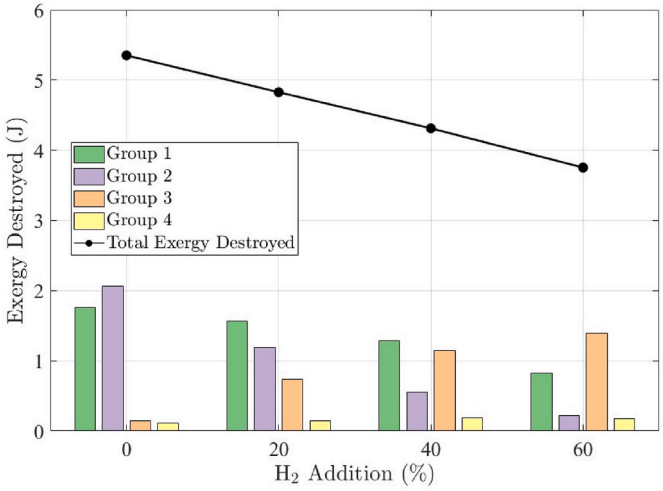

Fig. 6. Total destroyed exergy and its division into four main groups during the autoignition of ammonia mixtures with various hydrogen addition percentages (P = 5 MPa, T_{in} = 900 K, ∅ = 1).

89% for hydrogen addition percentages, respectively. It could be seen from Fig. 6 that the exergy destruction from radical growth reactions (group 3) increase by approximately by 424%, 707%, and 885% for hydrogen addition percentages of 20%, 40%, and 60%, respectively. In contrast, the exergy destruction from ammonia fuel fragmentation (group 1) reactions decreases by approximately 11%, 27%, and 53% for 20%, 40%, and 60% hydrogen addition percentage, respectively. This was due to the shift from ammonia oxidation towards the hydrogen oxidation. As also shown in the IDT sensitivity analysis with hydrogen addition to ammonia mixtures the H-atom abstractions shift away of NNH decomposition. So, there is a trade-off with increasing hydrogen addition between the slower, irreversible exergy destruction from fuel fragmentation and NH_X–NO_X chemistry (Groups 1 and 2) and the faster, more efficient radical propagation reactions (Group 3). Finally, it can be seen that the fourth group represents radical termination reactions did not vary significantly with hydrogen addition to ammonia. These findings suggest that as the cumulative exergy destruction of ammonia decreases by up to 30% with 60% hydrogen addition, less exergy is lost due to the irreversible chemical processes associated with autoignition. Based on the second law of thermodynamics, the reduction in entropy generation during ammonia autoignition with higher hydrogen addition means that a greater proportion of the fuel's exergy is available for useful work. Moreover, hydrogen addition significantly decreases the ammonia autoignition delay time, which could indicate a reduction in cycle-to-cycle variation, a challenging characteristic of ammonia ICE due to the low reactivity of ammonia [35].

3.3.2. *Effect of equivalence ratio*

The equivalence ratio significantly influences combustion temperature and the associated thermodynamic irreversibilities. Operating at leaner mixtures reduces the temperature, which in turn increases the rate of combustion irreversibility. As shown in Fig. 7, the ratio of exergy destroyed to the chemical potential for ammonia with different hydrogen addition percentages under various equivalence ratios is presented. For neat ammonia, the fraction of chemical potential destroyed due to autoignition increased from 13% to 14%, 17%, and 21% as the equivalence ratio decreased from 1.0 to 0.9, 0.7, and 0.5, respectively. The rise in combustion irreversibility is directly proportional to the rate of entropy generation. Overall, as air dilution increases the entropy generation increases due to an increase in the chemical entropy of the combustion products. Although lean mixtures reduces the product temperature and the sensible entropy component, the presence of excess air increases the number and distribution of product species, resulting in higher total entropy generation [36]. Fig. 8 also shows the ratio of each reaction group defined in Section 3.2 to the total chemical potential of ammonia at various equivalence ratios. Overall, a decrease in the mixture equivalence ratio led to an increase in all sub-divided groups, primarily due to the reduced fuel concentration in the reactor mixture. For neat ammonia, the contributions from fuel initiation and decomposition reactions, as well as NH_X oxidation and NO_X chemistry, increased significantly from 4% to 5% to 7% and 9%, respectively. For

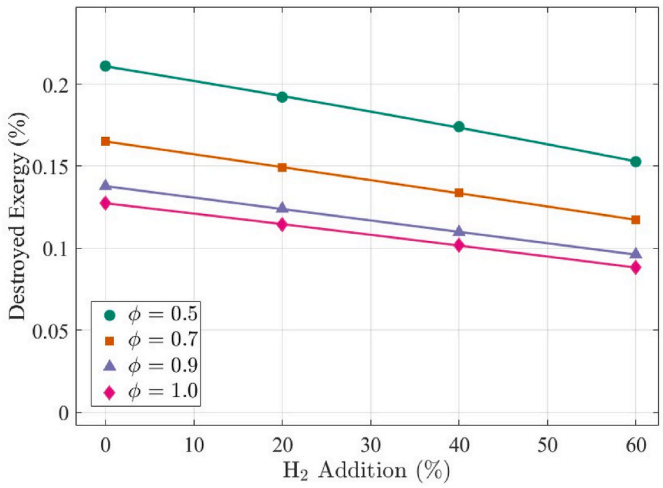

Fig. 7. Ratio of exergy destroyed to chemical potential for ammonia mixtures with different hydrogen addition percentages at various equivalence ratios ($P = 5$ MPa, $T_{in} = 900$ K).

ammonia with 60% hydrogen addition, Group 3 showed the greatest increase as the equivalence ratio was reduced from 1.0 to 0.5. This occurs because hydrogen addition enhances the ignition characteristics of the ammonia mixture. As discussed in Section 3.1, the chain-branching reaction $H+O_2=O+OH$ is the main ignition promoter. Furthermore, the reverse reaction $NH_3+H=NH_2+H_2$ increases the accumulation of H atoms, which further enhances reactivity through the chain-branching pathway $H+O_2=O+OH$ [8]. It can be observed that higher hydrogen addition to ammonia results in a more favourable exergy distribution, as a larger fraction of the exergy is destroyed through OH formation reactions that are beneficial for ignition. In particular, the enhanced contribution of chain-branching and radical propagation reactions that promote exergy destruction is increasingly associated with productive reaction pathways that accelerate heat release and improve mixture reactivity. Overall, the effect of hydrogen addition on ammonia exergy destroyed by autoignition follows a consistent trend across all equivalence ratios: exergy destruction from radical growth reactions (Group 3) increase with hydrogen addition, while exergy destruction from fuel fragmentation (Group 1), NH_X–NO_X chemistry (Group 2) decrease, and radical termination reactions (Group 4) remain largely unaffected.

4. Conclusion

This study evaluates the exergy destruction during the autoignition of ammonia-hydrogen mixtures in a constant-volume chamber by quantifying the exergy destruction associated with each elementary reaction using species production rates and corresponding Gibbs free energy changes and key conclusions are:

- For neat ammonia autoignition at elevated pressure, the most significant reactions promoting reactivity are $NH_2+NO_2=H_2NO+NO$ and $H_2NO+O_2=N_2+H_2O$, while the dominant reaction inhibiting reactivity is $NH_2+NO=N_2+H_2O$. Hydrogen addition shifts the dominant pathways away from NH_x oxidation toward chain-branching reactions such as $H_2O_2(+M)=2OH(+M)$.
- Hydrogen addition increases the instantaneous exergy destruction rate due to enhanced radical generation and accelerated chain-branching reactions, yet reduces cumulative exergy destruction by 19% and 30% for 40% and 60% hydrogen addition, respectively, primarily due to the shorter ignition delay time which reduces the duration available for irreversible processes.
- Overall, hydrogen addition follows a consistent pattern across the four reaction groups: exergy destruction from fuel fragmentation (Group 1) and NH_X–NO_X chemistry (Group 2) decrease, while exergy destruction from radical growth reactions (Group 3) increase due to

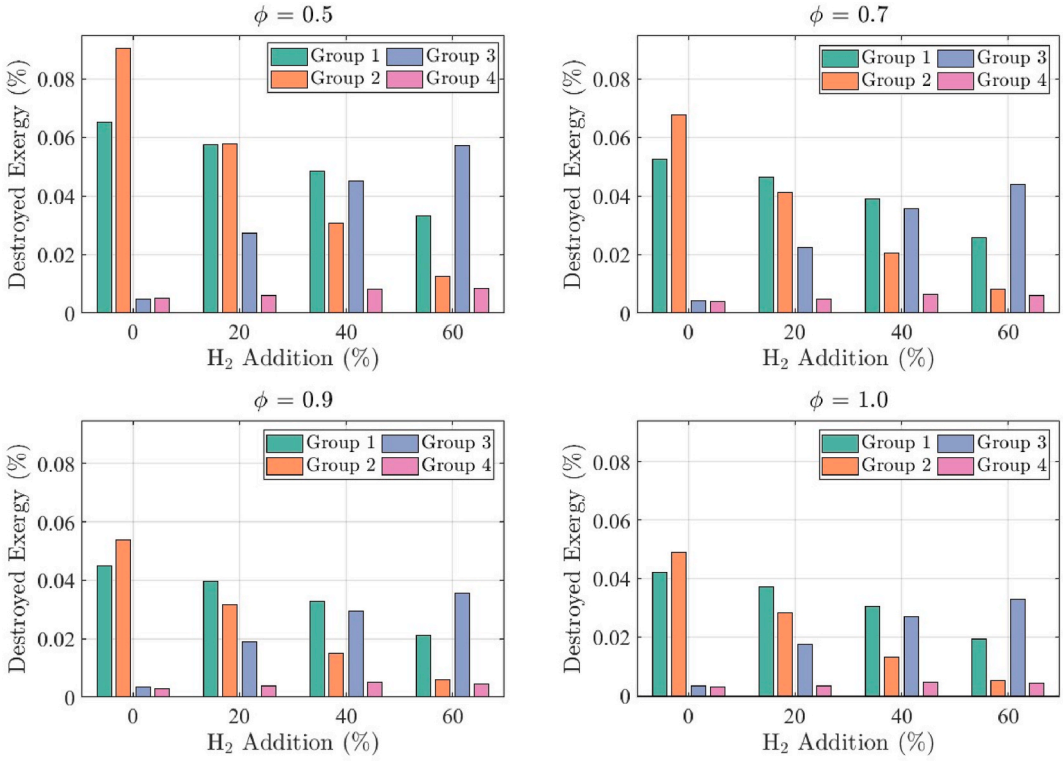

Fig. 8. Ratio of exergy destroyed by reactions from Group 1 to 4 to chemical potential for ammonia mixtures with different hydrogen addition percentages at various equivalence ratios ($P = 5$ MPa, $T_{in} = 900$ K).

enhanced OH and H production, and radical termination reactions (Group 4) remain largely unaffected.

These results provide fundamental mechanisms into the thermodynamic irreversibility of ammonia with hydrogen autoignition process and demonstrate the potential of hydrogen addition to improve ignition efficiency by reducing overall exergy destruction. This study provides a fundamental understanding of exergy destruction during the autoignition process of ammonia with hydrogen mixtures, the results remain largely theoretical, as they assume homogeneous, adiabatic, and constant-volume combustion under constant internal energy conditions. In reality, combustion occurs within an engine cylinder where both internal energy and volume vary with crank angle position. Therefore, extending the second law of thermodynamics analysis to a full engine simulation represents a valuable direction for future work.

CRediT authorship contribution statement

D.N. Rrustemi: Conceptualization, Investigation, Methodology, Writing – original draft. **T. Megaritis:** Conceptualization, Funding acquisition, Investigation, Project administration, Resources, Supervision, Writing – review & editing. **L.C. Ganippa:** Formal analysis, Investigation, Methodology, Project administration, Supervision, Writing – review & editing.

Declaration of competing interest

The authors declare that they have no known competing financial interests or personal relationships that could have appeared to influence the work reported in this paper.

Acknowledgements

We acknowledge the financial support of Engineering and Physical Sciences Research Council (EPSRC) of the UK under Grant No. EP/X019578/1.

References

[1] Madheswaran DK, Vengatesan S, Jegadheeswaran S, Thangamuthu M, Togun H, Duraisamy B, et al. Ammonia as a hydrogen carrier: a comprehensive analysis of electrolysis efficiency and its potential in sustainable energy systems. Renew Sustain Energy Rev 2025;221:115915. https://doi.org/10.1016/j.rser.2025.115915.

[2] Sun J, Zhao N, Zheng H. A comprehensive review of ammonia combustion: fundamental characteristics, chemical kinetics, and applications in energy systems. Fuel 2025;394:135135. https://doi.org/10.1016/j.fuel.2025.135135.

[3] Han D, Liu Y, Huang Z. The use of ammonia as a fuel for combustion engines. In: Kalghatgi G, Agarwal AK, Leach F, Senecal K, editors. Engines and fuels for future transport. Singapore: Springer Singapore; 2022. C1. https://doi.org/10.1007/978-981-16-8717-4_16. C1.

[4] Masoumi S, Ashjaee M, Houshfar E. Laminar flame stability analysis of ammonia-methane and ammonia-hydrogen dual-fuel combustion. Fuel 2024;363:131041. https://doi.org/10.1016/j.fuel.2024.131041.

[5] Rrustemi DN, Megaritis T, Ganippa LC. Modelling hydrogen enriched ammonia combustion through laminar flame speed and mass fraction burn analysis. Fuel 2026;422:139124. https://doi.org/10.1016/j.fuel.2026.139124.

[6] Zhang F, Zhang G, Wang Z, Wu D, Jangi M, Xu H. Experimental investigation on combustion and emission characteristics of non-premixed ammonia/hydrogen flame. Int J Hydrog Energy 2024;61:25–38. https://doi.org/10.1016/j.ijhydene.2024.02.281.

[7] Gotama GJ, Hayakawa A, Okafor EC, Kanoshima R, Hayashi M, Kudo T, et al. Measurement of the laminar burning velocity and kinetics study of the importance of the hydrogen recovery mechanism of ammonia/hydrogen/air premixed flames. Combust Flame 2022;236:111753. https://doi.org/10.1016/j.combustflame.2021.111753.

[8] Otomo J, Koshi M, Mitsumori T, Iwasaki H, Yamada K. Chemical kinetic modeling of ammonia oxidation with improved reaction mechanism for ammonia/air and ammonia/hydrogen/air combustion. Int J Hydrog Energy 2018;43:3004–14. https://doi.org/10.1016/j.ijhydene.2017.12.066.

[9] Zhu Y, Curran HJ, Girhe S, Murakami Y, Pitsch H, Senecal K, et al. The combustion chemistry of ammonia and ammonia/hydrogen mixtures: a comprehensive chemical kinetic modeling study. Combust Flame 2024;260:113239. https://doi.org/10.1016/j.combustflame.2023.113239.

[10] Baker JB, Rahman RK, Pierro M, Higgs J, Urso J, Kinney C, et al. Experimental ignition delay time measurements and chemical kinetics modeling of Hydrogen/Ammonia/Natural gas fuels. J Eng Gas Turbines Power 2023;145:041002. https://doi.org/10.1115/1.4055721.

[11] Mathieu O, Petersen EL. Experimental and modeling study on the high-temperature oxidation of Ammonia and related NOx chemistry. Combust Flame 2015;162:554–70. https://doi.org/10.1016/j.combustflame.2014.08.022.

[12] Chen J, Jiang X, Qin X, Huang Z. Effect of hydrogen blending on the high temperature auto-ignition of ammonia at elevated pressure. Fuel 2021;287:119563. https://doi.org/10.1016/j.fuel.2020.119563.

[13] Reitz RD, Ogawa H, Payri R, Fansler T, Kokjohn S, Moriyoshi Y, et al. IJER editorial: the future of the internal combustion engine. Int J Engine Res 2020;21:3–10. https://doi.org/10.1177/1468087419877990.

[14] Caton JA. A review of investigations using the second law of thermodynamics to Study internal-combustion engines. SAE World Congress; 2000. https://doi.org/10.4271/2000-01-1081.

[15] Caton JA. Exergy destruction during the combustion process as functions of operating and design parameters for a spark-ignition engine. Int J Energy Res 2012;36:368–84. https://doi.org/10.1002/er.1807.

[16] Rakopoulos C, Giakoumis E. Second-law analyses applied to internal combustion engines operation. Prog Energy Combust Sci 2006;32:2–47. https://doi.org/10.1016/j.pecs.2005.10.001.

[17] Nishida K, Takagi T, Kinoshita S. Analysis of entropy generation and exergy loss during combustion. Proc Combust Inst 2002;29:869–74. https://doi.org/10.1016/S1540-7489(02)80111-0.

[18] Acampora L, Marra FS. Second law thermodynamic analysis of syngas premixed flames. Int J Hydrog Energy 2020;45:12185–202. https://doi.org/10.1016/j.ijhydene.2020.02.142.

[19] Zhang Z, Kalaycı N, Lou C, Cai W. Numerical analysis of radiative and energy conversion for ammonia/hydrogen-air premixed flame in a planar micro-combustor. Fuel 2025;400:135734. https://doi.org/10.1016/j.fuel.2025.135734.

[20] Feng H, Wang X, Zhang J. Study on the effects of intake conditions on the exergy destruction of low temperature combustion engine for a toluene reference fuel. Energy Convers Manag 2019;188:241–9. https://doi.org/10.1016/j.enconman.2019.02.090.

[21] Wu H, Liu Y, Sun W, Huang Z, Zhang Y. Exergy destruction behavior of chemical reactions during the auto-ignition of methane doped with hydrogen. Int J Hydrog Energy 2024;57:869–79. https://doi.org/10.1016/j.ijhydene.2023.12.160.

[22] Gersen S, Anikin N, Mokhov A, Levinsky H. Ignition properties of methane/hydrogen mixtures in a rapid compression machine. Int J Hydrog Energy 2008;33:1957–64. https://doi.org/10.1016/j.ijhydene.2008.01.017.

[23] Zhang J, Huang Z, Han D. Exergy losses in auto-ignition processes of DME and alcohol blends. Fuel 2018;229:116–25. https://doi.org/10.1016/j.fuel.2018.04.162.

[24] Zhang J, Huang Z, Min K, Han D. Dilution, thermal, and chemical effects of carbon dioxide on the exergy destruction in *n* -Heptane and iso-octane autoignition processes: a numerical study. Energy Fuels 2018;32:5559–70. https://doi.org/10.1021/acs.energyfuels.7b04018.

[25] Som SK, Datta A. Thermodynamic irreversibilities and exergy balance in combustion processes. Prog Energy Combust Sci 2008;34:351–76. https://doi.org/10.1016/j.pecs.2007.09.001.

[26] Rrustemi DN, Ganippa LC, Axon CJ. Exergy analysis of the lean-burn hydrogen-fuelled engine. Energy 2025;314:134110. https://doi.org/10.1016/j.energy.2024.134110.

[27] Methling T, Pierro M, Hulliger N, Urso JJ, Krämer J, Naumann C, et al. Experimental investigation and optimization of ammonia–hydrogen chemical kinetics with ignition delay times from shock tubes. Proc Combust Inst 2025;41:105835. https://doi.org/10.1016/j.proci.2025.105835.

[28] Shrestha KP, Lhuillier C, Barbosa AA, Brequigny P, Contino F, Mounaïm-Rousselle C, et al. An experimental and modeling study of ammonia with enriched oxygen content and ammonia/hydrogen laminar flame speed at elevated pressure and temperature. Proc Combust Inst 2021;38:2163–74. https://doi.org/10.1016/j.proci.2020.06.197.

[29] Girhe S, Snackers A, Lehmann T, Langer R, Loffredo F, Glaznev R, et al. Ammonia and ammonia/hydrogen combustion: comprehensive quantitative assessment of kinetic models and examination of critical parameters. Combust Flame 2024;267:113560. https://doi.org/10.1016/j.combustflame.2024.113560.

[30] Liang W, Law CK. Enhancing ammonia combustion using reactivity stratification with hydrogen addition. Proc Combust Inst 2023;39:4419–26. https://doi.org/10.1016/j.proci.2022.10.025.

[31] Pierro M, Dennis CW, Pothen A-A, Hulliker N, Kelly T, Fraze M, et al. Ammonia and Ammonia/Hydrogen mixtures ignition delay times and chemical kinetic model validation at gas turbine relevant conditions. ASME Turbo Expo; 2024. https://doi.org/10.1115/GT2024-129083.

[32] Hurault F, Fenard Y, Brequigny P, Moreau B, Haidous Y, Foucher F, et al. Experimental and numerical ignition delay times comparison for ammonia mechanisms at high pressure. Proc Combust Inst 2024;40:105625. https://doi.org/10.1016/j.proci.2024.105625.

[33] Yan Y, Liu Z, Liu J. Computational analysis of ammonia-hydrogen blends in homogeneous charge compression ignition engine operation. Process Saf Environ Prot 2024;190:1263–72. https://doi.org/10.1016/j.psep.2024.07.102.

[34] Wang Y, Zhou X, Liu L. Study on the mechanism of the ignition process of ammonia/hydrogen mixture under high-pressure direct-injection engine

conditions. Int J Hydrog Energy 2021;46:38871–86. https://doi.org/10.1016/j.ijhydene.2021.09.122.
[35] Huang Z, Zhu T, Wang L, Wang T, Chen H, Wang L. Effects of ammonia on cycle-by-cycle variations in a spark ignition engine fueled with hydrogen. Int J Hydrog Energy 2025;111:196–204. https://doi.org/10.1016/j.ijhydene.2025.02.192.
[36] Knizley AA, Srinivasan KK, Krishnan SR, Ciatti SA. Fuel and diluent effects on entropy generation in a constant internal energy–volume (uv) combustion process. Energy 2012;43:315–28. https://doi.org/10.1016/j.energy.2012.04.024.